



Article

Comparison of Oleocanthal-Low EVOO and Oleocanthal against Amyloid- β and Related Pathology in a Mouse Model of Alzheimer's Disease

Ihab M. Abdallah ¹, Kamal M. Al-Shami ¹ , Amer E. Alkhalifa ¹, Nour F. Al-Ghraiya ¹, Claudia Guillaume ² and Amal Kaddoumi ^{1,*} 

¹ Department of Drug Discovery and Development, Harrison College of Pharmacy, Auburn University, 720 S Donahue Dr., Auburn, AL 36849, USA

² Modern Olives, 151 Broderick Road, Lara, VIC 3212, Australia

* Correspondence: kaddoumi@auburn.edu

Abstract: Alzheimer's disease (AD) is characterized by several pathological hallmarks, including the deposition of amyloid- β (A β) plaques, neurofibrillary tangles, blood–brain barrier (BBB) dysfunction, and neuroinflammation. Growing evidence support the neuroprotective effects of extra-virgin olive oil (EVOO) and oleocanthal (OC). In this work, we aimed to evaluate and compare the beneficial effects of equivalent doses of OC-low EVOO (0.5 mg total phenolic content/kg) and OC (0.5 mg OC/kg) on A β and related pathology and to assess their effect on neuroinflammation in a 5xFAD mouse model with advanced pathology. Homozygous 5xFAD mice were fed with refined olive oil (ROO), OC-low EVOO, or OC for 3 months starting at the age of 3 months. Our findings demonstrated that a low dose of 0.5 mg/kg EVOO-phenols and OC reduced brain A β levels and neuroinflammation by suppressing the nuclear factor- κ B (NF- κ B) pathway and reducing the activation of NOD-, LRR- and pyrin domain-containing protein 3 (NLRP3) inflammasomes. On the other hand, only OC suppressed the receptor for advanced glycation endproducts/high-mobility group box 1 (RAGE/HMGB1) pathway. In conclusion, our results indicated that while OC-low EVOO demonstrated a beneficial effect against A β -related pathology in 5xFAD mice, EVOO rich with OC could provide a higher anti-inflammatory effect by targeting multiple mechanisms. Collectively, diet supplementation with EVOO or OC could prevent, halt progression, and treat AD.

Keywords: olive oil; EVOO; oleocanthal; amyloid β ; neuroinflammation; NLRP3 inflammasome; RAGE; NF- κ B pathway; Alzheimer's disease



Citation: Abdallah, I.M.; Al-Shami, K.M.; Alkhalifa, A.E.; Al-Ghraiya, N.F.; Guillaume, C.; Kaddoumi, A. Comparison of Oleocanthal-Low EVOO and Oleocanthal against Amyloid- β and Related Pathology in a Mouse Model of Alzheimer's Disease. *Molecules* **2023**, *28*, 1249. <https://doi.org/10.3390/molecules28031249>

Academic Editors: Lorenzo Cecchi and Maria Bellumori

Received: 15 December 2022

Revised: 6 January 2023

Accepted: 25 January 2023

Published: 27 January 2023



Copyright: © 2023 by the authors. Licensee MDPI, Basel, Switzerland. This article is an open access article distributed under the terms and conditions of the Creative Commons Attribution (CC BY) license (<https://creativecommons.org/licenses/by/4.0/>).

1. Introduction

Alzheimer's disease (AD) is a progressive neurodegenerative disorder and is the most common type of dementia [1]. Approximately 10% of individuals over 65 years have AD, and its incidence continues to increase with age [2]. Clinical symptoms of AD include progressive memory deficits, cognitive dysfunction, and motor abnormalities, which could ultimately affect executive function, speech, and visuospatial orientation [2,3]. AD is characterized by two key pathological hallmarks, namely, the extracellular deposition of amyloid- β (A β) plaques and neurofibrillary tangles (NFTs) [4–7]. A β pathology results from the cleavage of the amyloid precursor protein (APP); APP is a membrane-bound protein that is processed to produce A β peptides such as A β ₄₀ and A β ₄₂ [8]. Produced A β monomers aggregate to form intermediate structures called A β oligomers, which eventually aggregate to form A β fibrils and plaques, thus contributing to AD pathology [9].

While A β deposition and the intraneuronal deposits of NFTs are the key players in the pathological characteristics of AD [10], they alone cannot elucidate AD's pathogenesis, suggesting the involvement of additional pathways involved in AD pathological process [11].

Accumulating evidence supports neuroinflammation's role in the progression of the neuropathological changes observed in AD [12–14]. In the initial stages of AD, glial cells positively affect A β elimination by phagocytosis [15]. However, upon chronic exposure to increased A β levels, both astrocytes and microglia become reactive, hence, activating several inflammatory pathways such as the NOD-, LRR- and pyrin domain-containing protein 3 (NLRP3) inflammasomes and receptor for advanced glycation endproducts/high mobility group box 1 (RAGE/HMGB1) pathways [16,17]. The continuous activation of astrocytes and microglia leads to changes in their phenotypes and morphology accompanied by elevated secretion of proinflammatory cytokines such as interleukin-6 (IL-6) and interleukin-1 β (IL-1 β) [18,19].

Moreover, the accumulation of A β and neuroinflammation leads to blood–brain barrier (BBB) dysfunction [20]. BBB consists of several cellular components, including endothelial cells, astrocytes, pericytes, and basement membranes [21]. The endothelial cells of the BBB are tightly connected through tight and adherence junction proteins. This tight connection restricts solute movement between the blood and the brain [21]. A key route for A β clearance from the brain is through its transport across the BBB, mediated by A β key transport proteins P-glycoprotein (P-gp) and the low-density lipoprotein receptor-related protein-1 (LRP1) [22–24]. Both tight and adherence junctions and transport proteins are downregulated in AD [21–24].

Several studies demonstrated the beneficial effect of the Mediterranean diet in halting and slowing AD progression [25,26]. One integral component of the Mediterranean diet that has been evaluated for its health-promoting impact is extra-virgin olive oil (EVOO). EVOO has been studied extensively for its promising health benefits. Several studies have revealed that EVOO slows memory impairment progression and improves cognitive performance in humans and AD mouse models [27–33]. Moreover, our studies have shown that the addition of EVOO to the diet of AD mouse models enhanced the BBB function, increased A β clearance, reduced its production, and reduced neuroinflammation [29–31]. EVOO is composed of glycerol (~95%) and nonglycerol (~5%) and is obtained from the first pressing of the olive fruit by mechanical means [34]. EVOO contains more than 35 phenolic compounds possessing many antioxidant and anti-inflammatory characteristics [35–37]. Among the phenolic compounds that were isolated and characterized is oleocanthal (OC) [37]. Oleocanthal proved effective against A β and related pathology in AD mouse models [28–31,38]. At 5 and 10 mg/kg doses, OC reduced brain A β levels, improved BBB function, and reduced neuroinflammation [28,38]. In separate studies, we evaluated the effect of OC-low and OC-rich EVOO on A β and related pathology in AD mouse models; both olive oils demonstrated neuroprotective effects [30,31,38].

Besides OC, EVOO contains several phenolic compounds such as hydroxytyrosol, tyrosol, oleuropein, and oleacein, to list a few, which also demonstrated neuroprotective effects when tested *in vitro* and *in vivo* [39–48]. Different grades of olive oil are available based on the phenolic content, including phenolic-free refined olive oil (ROO), phenolic-rich EVOO (but low in OC), and OC-rich EVOO. Yet, a direct comparison between these olive oils for their neuroprotective effect has not been evaluated, which is essential to clarify the impact of EVOO with different phenolics content on AD pathology. Thus, in this work, we aimed to assess and compare the effect of ROO, OC-low EVOO- and OC-enriched diet added at a low dose of 0.5 mg/kg body weight per day for three months on brain A β levels and neuroinflammation in a homozygous 5xFAD mouse model of AD.

2. Results

2.1. EVOO and OC Treatments Reduced A β Burden in 5xFAD Mouse Brains

Homozygous 5xFAD mice were fed with refined olive oil (ROO), OC-low EVOO (0.5 mg total phenolic content/kg; hereafter EVOO), and OC (0.5 mg OC/kg) for 3 months starting at the age of 3 months. Compared to ROO-treated mice, EVOO and OC treatments reduced total A β load in 5xFAD mouse brains as determined by immunofluorescence analysis. As shown in Figure 1A, EVOO and OC treatments reduced total A β (detected

by 6E10 antibody) levels in brain sections. In addition, both EVOO and OC reduced A β plaques as determined by Thioflavin S (ThioS) staining (Figure 1B). Further analysis was performed to evaluate the effect of treatments on the levels of soluble A β_{40} and A β_{42} by ELISA (Figure 1C). Compared to the ROO group, EVOO significantly reduced A β_{42} by 35%; however, it didn't reach significance for its effect on A β_{40} levels, which decreased by 30% due to the high variability in the ROO group; OC, on the other hand, was able to reduce both isoforms significantly by about 50%. While no significant difference was observed between EVOO and OC on reduced A β_{40} levels, OC demonstrated a significant reduction in A β_{42} levels compared to EVOO.

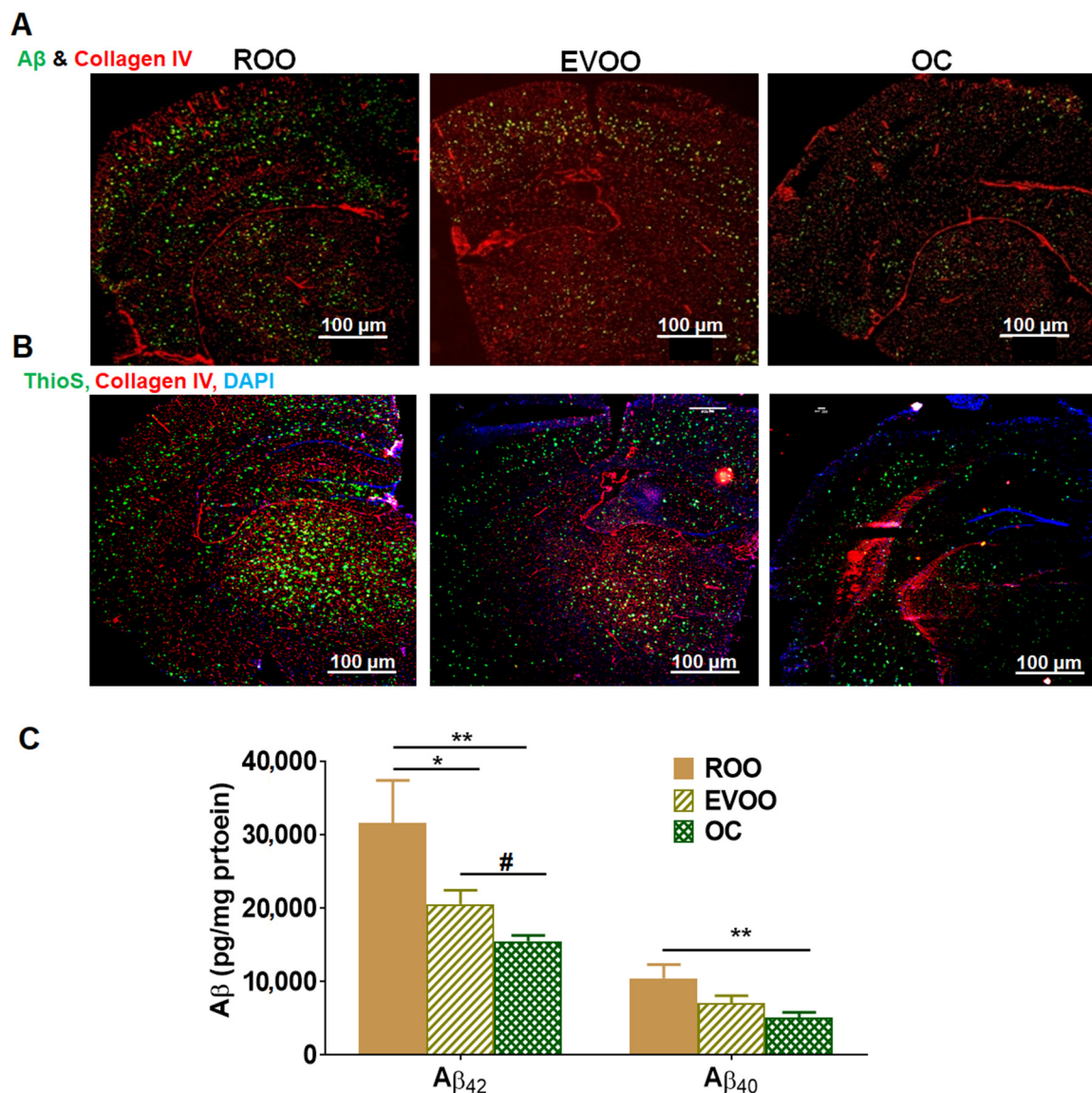


Figure 1. Effect of EVOO and OC consumption (0.5 μ g/kg) for three months on A β burden in 5xFAD mouse brains. (A) Representative brain sections stained with 6E10 antibody to detect total A β load and anti-collagen IV antibody to detect microvessels. (B) Representative brain sections stained with ThioS to detect A β plaques, anti-collagen IV antibody to detect microvessels, and DAPI (blue). Scale bar, 100 μ m. (C) Brain levels of both soluble human A β_{40} and A β_{42} levels were determined by ELISA. Data represented as mean \pm SEM (n = 8 mice per group). * $p < 0.05$, ** $p < 0.01$ compared to ROO; # $p < 0.05$ compared to EVOO.

2.2. EVOO and OC Enhanced BBB Function in 5xFAD Mice Brains

To monitor and compare the effect of EVOO and OC on the BBB function, we evaluated their effect on the expression of A β major transport proteins P-gp and LRP1, the tight junction proteins claudin-5 and occludin, and the adherence junction protein VE-cadherin by Western blot. As shown in Figure 2A, EVOO and OC increased the expression of P-gp by 33%–39% compared with ROO-treated mice. For their effect on LRP1, while the effect was mild, both EVOO and OC significantly increased LRP1 levels by 17% and 25%, respectively.

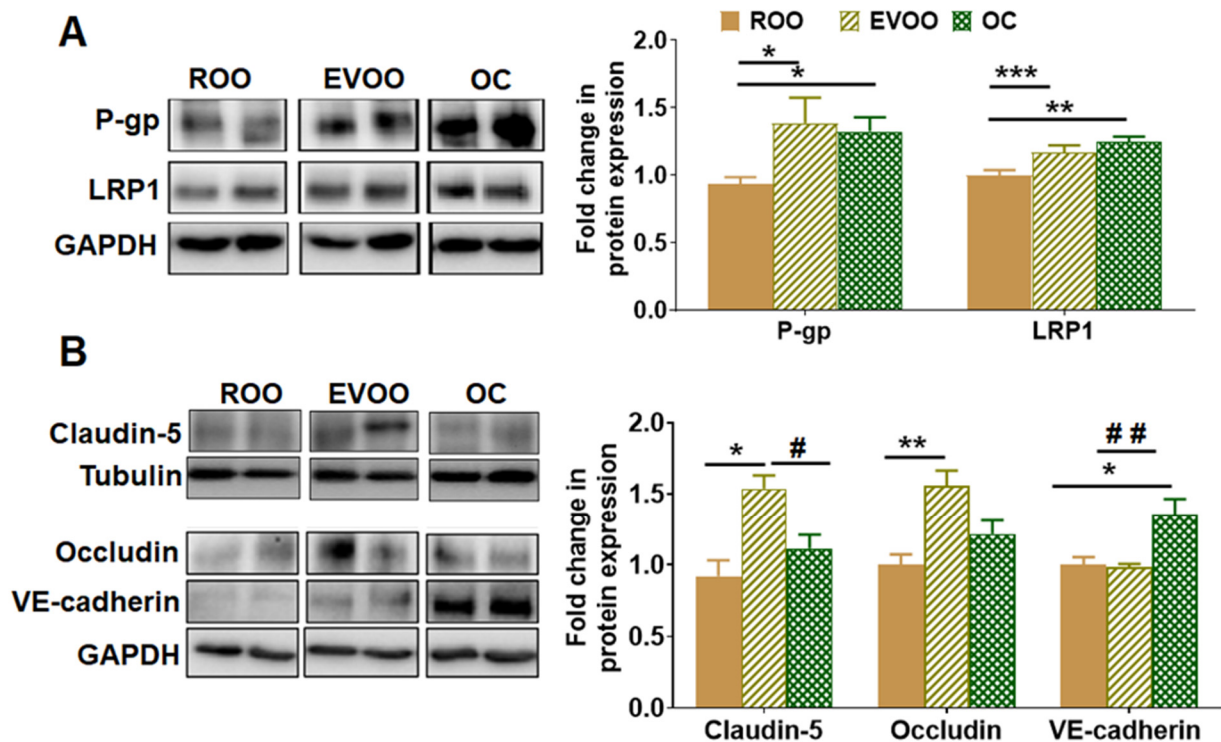


Figure 2. Effect of EVOO and OC consumption (0.5 μ g/kg) for three months on A β clearance, and tight and adherence junction proteins in 5xFAD mouse brains. (A) Representative blots and densitometry analysis of A β major transport proteins across the BBB, P-gp, and LRP1. (B) Representative blots and densitometry analysis of the tight junction proteins claudin-5 and occludin and the adherence protein VE-cadherin (n = 6–8 mice per group). Values were normalized to the ROO group (1.0). Data are presented as mean \pm SEM. * $p < 0.05$, ** $p < 0.01$, *** $p < 0.001$ compared to ROO; and # $p < 0.05$, ## $p < 0.01$ compared to EVOO.

Regarding their effect on tight and adherence junction proteins, EVOO significantly increased claudin-5 and occludin expressions by 44% and 56%, respectively, while OC increased VE-cadherin significantly by 35% (Figure 2B).

2.3. EVOO and OC Reduced the Amyloidogenic and Enhanced the Non-Amyloidogenic Pathways in 5xFAD Mouse Brains

The effect of EVOO and OC on A β production was evaluated by monitoring changes in the expression of sAPP α , sAPP β , and ADAM10 (α -secretase) by Western blot. APP processing undergoes enzymatic cleavages by ADAM10 to produce sAPP α (the non-amyloidogenic pathway) and by β -secretase to produce sAPP β followed by γ -secretase cleavage to form A β peptides (the amyloidogenic pathway). As shown in Figure 3, the consumption of EVOO- and OC-enriched diet significantly increased the expression of ADAM10 by approximately 35% compared with the ROO group. This increase was associated with a significant increase in sAPP α by 25% in mice that consumed EVOO and OC brains. In

addition, EVOO and OC significantly reduced sAPP β levels by 30%–40% (Figure 3). There was no significant difference between EVOO and OC in their effect on A β production.

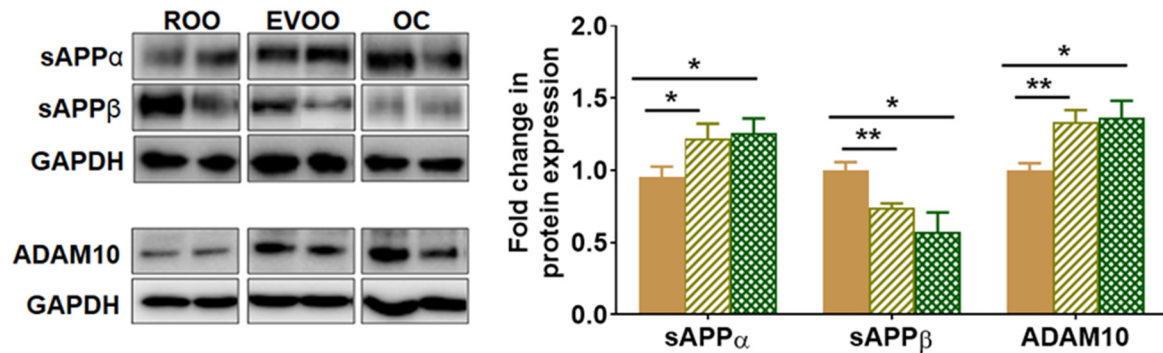


Figure 3. Effect of EVOO and OC consumption (0.5 $\mu\text{g}/\text{kg}$) for three months on A β production proteins in 5xFAD mouse brains. Representative blots and densitometry analysis of sAPP α , sAPP β , and ADAM10 (n = 6 mice per group). Values were normalized to the ROO group (1.0). Data are presented as mean \pm SEM. * $p < 0.05$, ** $p < 0.01$ compared to ROO.

2.4. EVOO and OC Increased the Expression of Synaptic Markers in 5xFAD Mouse Brains

Two pre-synaptic markers (SNAP-25 and synapsin-1) and one post-synaptic marker (PSD-95) were evaluated. As shown in Figure 4, Western blot findings demonstrated EVOO, and OC significantly increased the expression of the neurosynaptic markers PSD-95 by 2- and 2.5-fold, SNAP-25 by 1.5- and 2.9-fold, and synapsin-1 by 1.3 and 1.4-fold, respectively, when compared with the ROO enriched-diet. While both EVOO and OC induced the synaptic markers, OC demonstrated a significant increase in SNAP-25 expression compared with EVOO.

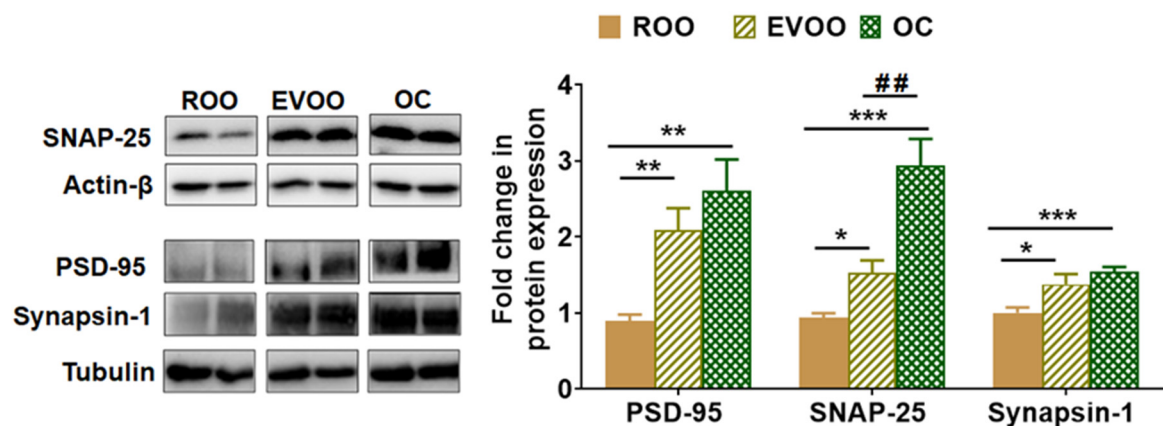


Figure 4. Effect of EVOO and OC consumption (0.5 $\mu\text{g}/\text{kg}$) for three months on synaptic markers in 5xFAD mouse brains. Representative blots and densitometry analysis of PSD-95, SNAP-25 and synapsin-1 (n = 6 mice per group). Values were normalized to the ROO group (1.0). Data are presented as mean \pm SEM. * $p < 0.05$, ** $p < 0.01$, *** $p < 0.001$ compared to ROO; and ## $p < 0.01$ compared to EVOO.

2.5. EVOO and OC Reduced Neuroinflammation in 5xFAD Mouse Brains

Astrocyte activation is recognized by increased glial fibrillary acidic protein (GFAP) with an elongated shape and thick branches. As shown in Figure 5A, in comparison to the ROO group, EVOO and OC significantly reduced astrocyte activation and ameliorated the astrocyte shape in mouse brains. Besides astrocytes activation, stimuli such as A β

and the proinflammatory cytokines IL-1 β and IL-6 activate NLRP3, which promotes the inflammasome complex formation. Thus, in this work, we evaluated and compared the effect of EVOO and OC on the production of proinflammatory cytokines by ELISA, and NLRP3 by Western blotting. As shown in Figure 5B, mice treated with EVOO and OC significantly reduced IL-1 β levels by approximately 70% and 40%, respectively, and reduced IL-6 levels by about 60% (Figure 5B). The results demonstrated that the effect of EVOO on reducing IL-1 β is significantly greater than OC.

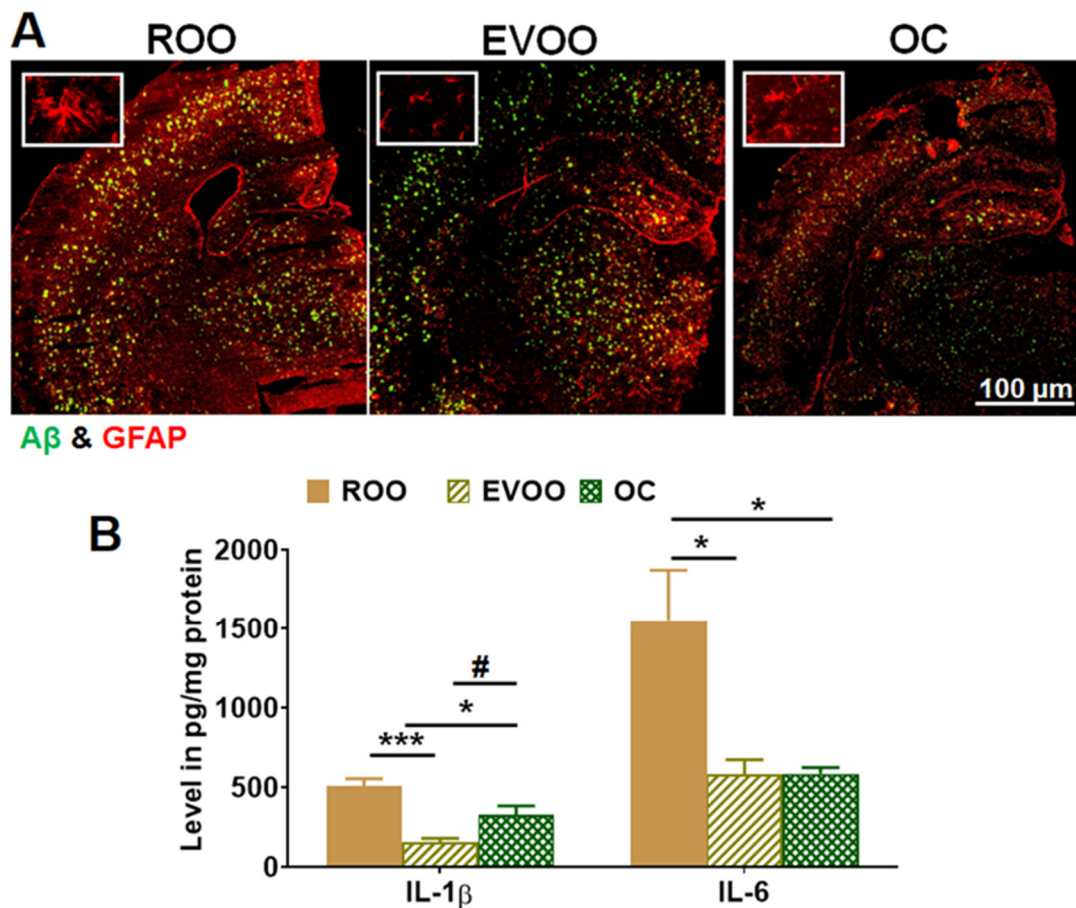


Figure 5. Effect of EVOO and OC consumption (0.5 μ g/kg) for three months on astrocytes activation and cytokines in 5xFAD mouse brains. (A) Representative brain sections stained with anti-GFAP antibody and anti-A β (6E10 antibody) to detect activated astrocytes (seen at higher magnification in the closed inserts, 500 μ m). (B) Brain levels of the cytokines IL-1 β and IL-6 as determined by ELISA (n = 6 mice per group). Values were normalized to the ROO group (1.0). Data are presented as mean \pm SEM. * $p < 0.05$, *** $p < 0.001$ compared to ROO; and # $p < 0.05$ compared to EVOO.

For their effect on NLRP3 inflammasome activation, OC demonstrated a significant reduction in NLRP3, pro-caspase 1, and pro-caspase 8 when compared to ROO and EVOO. As shown in Figure 6A, OC significantly reduced NLRP3 levels by 40% compared with the ROO group, while EVOO showed a 15% reduction. Reduced NLRP3 levels were associated with a significant decrease in pro-caspase 1 levels by 40% and 67% and pro-caspase 8 by 42% and 79% by EVOO and OC-treated mice, respectively.

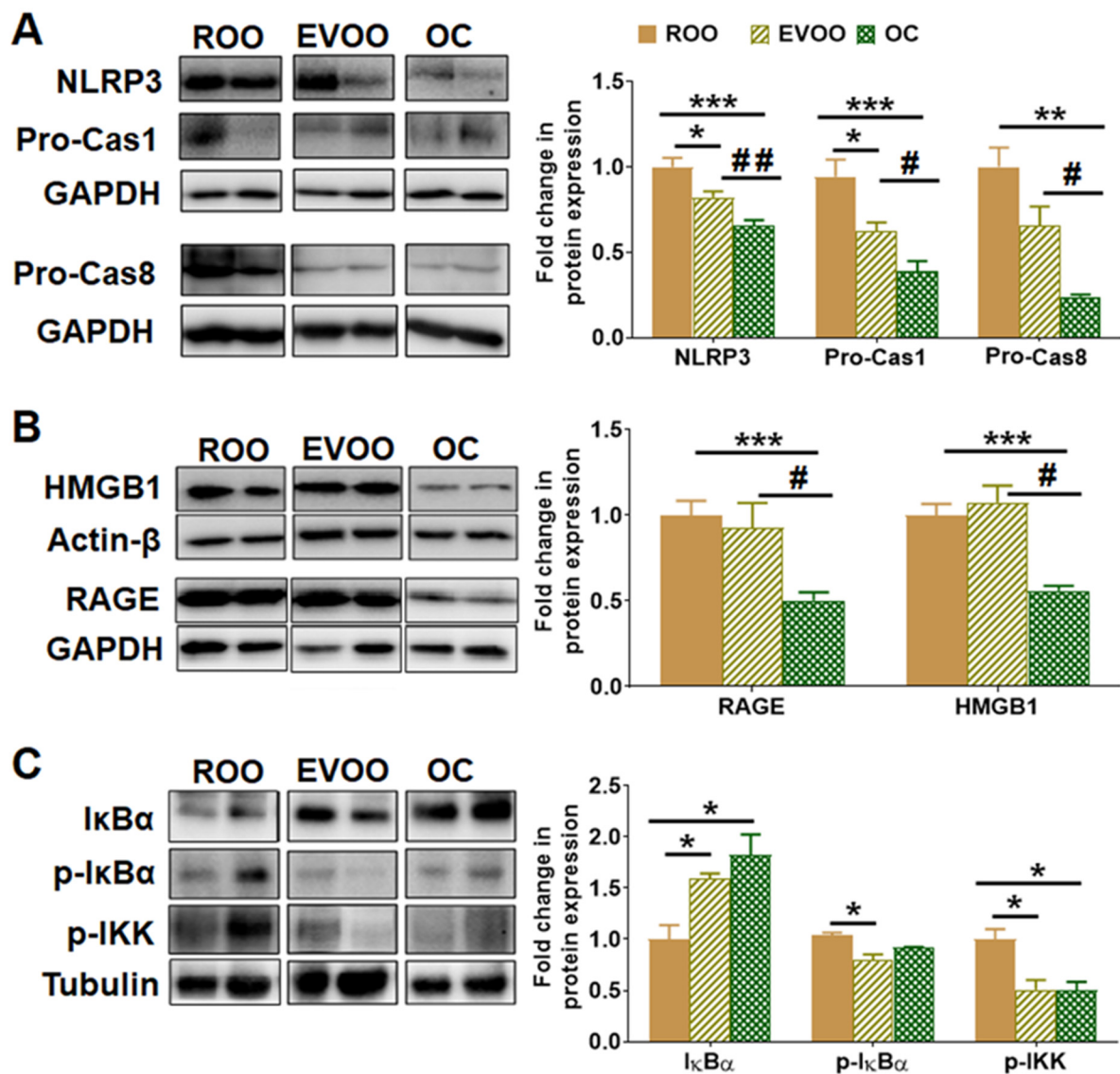


Figure 6. Effect of EVOO and OC consumption (0.5 μ g/kg) for three months on the neuroinflammation markers NLRP3, RAGE, and HMGB1, and NF- κ B pathway in 5xFAD mouse brains. (A) Representative blots and densitometry analysis of NLRP3, pro-caspase 1 (Pro-Cas1), and pro-caspase 8 (Pro-Cas8) in brain homogenates. (B) Representative blots and densitometry analysis of RAGE and HMGB1, and (C) Representative blots and densitometry analysis of I κ B α , p-I κ B α , and p-IKK α (n = 6–8 mice per group). Values were normalized to the ROO group (1.0). Data are presented as mean \pm SEM. * p < 0.05, ** p < 0.01, *** p < 0.001 compared to ROO; and # p < 0.05, ## p < 0.01 compared to EVOO.

2.6. OC Reduced RAGE and HMGB1 Expressions in 5xFAD Mouse Brains

Ligands, including A β and high-mobility group box protein 1 (HMGB1), interact with the receptor for AGEs (RAGE) and directly induce inflammation. Thus, we next examined EVOO and OC effects on the expression of RAGE and HMGB1 in the brain homogenates of the 5xFAD mice. As shown in Figure 6B, RAGE and HMGB1 expressions were significantly reduced by approximately 40%–50% by OC; however, EVOO did not alter the levels of either protein compared to the ROO group. These results suggest that besides suppressing NLRP3 inflammasomes, OC suppresses the RAGE/HMGB1 pathway.

2.7. EVOO- and OC-Reduced Neuroinflammation Is Mediated by NF- κ B Pathway in 5xFAD Mouse Brains

To determine whether the observed effect is mediated through attenuating NF- κ B pathway, we evaluated the impact of the treatments on three major proteins from the NF- κ B pathway, namely I κ B α , p-I κ B α (Ser32), and p-IKK β . As shown in Figure 6C, EVOO and OC significantly increased the expression of total I κ B α by approximately 60% and 80%, respectively, and both reduced the expression of p-IKK β by 50% compared with the ROO group. This significant reduction in p-IKK β was associated with a significant decrease in p-I κ B α by approximately 20% in the EVOO group; however, the effect of OC did not reach a significant level. The results also demonstrated no significant difference between EVOO and OC on the NF- κ B pathway, which suggests that EVOO and OC effect could be mediated, at least in part, by suppressing the NF- κ B pathway.

3. Discussion

AD is a complex neurodegenerative disorder that could be affected by modifiable and non-modifiable risk factors, thus influencing the disease susceptibility [49]. AD has several hallmarks, including A β plaques, NFT, compromised BBB, widespread activated glial cells, synaptic dysfunction, neuroinflammation, and neuronal death [4–7,10,14].

The Mediterranean diet has several beneficial effects and has been associated with a slower rate of cognitive impairment and dementia [50,51]. Olive oil is the primary fat source in the Mediterranean diet, which possesses anti-inflammatory, antioxidant, and neuroprotective effects [25–27,52]. Several studies by us and others have reported the beneficial effects of EVOO and its phenolic components, especially OC, in AD mouse models [28–31,38,53,54]. Previous findings from separate studies demonstrated that treating AD mouse models with OC-rich EVOO or high doses of OC (in saline as a vehicle) reduced A β and related pathology [28,30,31,38]. In addition, a few studies have tested the effect of EVOO in subjects with mild cognitive impairment (MCI) and reported the beneficial effect of EVOO containing variable phenolic content. EVOO consumption modulated plasma A β and hyperphosphorylated tau levels, enhanced the BBB function, reduced blood inflammatory and oxidative stress biomarkers, and improved cognitive function in MCI [32,33,55]. However, a direct comparison between OC-low EVOO and OC has not been assessed. Thus, in this study, we aimed to evaluate and compare the effect of equivalent doses of OC (spiked in ROO as the vehicle) and EVOO phenolic content present in OC-low EVOO on brain A β levels and neuroinflammation in homozygous 5xFAD mice characterized with aggressive A β pathology at an early age. Our findings from this work demonstrated the following: (a) feeding mice with OC-low EVOO- or OC-enriched diet reduced brain A β levels, astrocytes activation, and neuroinflammation, (b) at the administered low doses, both EVOO (0.5 mg phenolic content/kg) and OC (0.5 mg/kg) demonstrated comparable effects, (c) the anti-inflammatory effect of EVOO and OC is mediated, at least in part, by suppressing NF- κ B pathway and NLRP3 inflammasome activation; however, only OC suppressed RAGE/HMGB1 pathway, which infers that OC could possess a greater effect against neuroinflammation compared with EVOO.

Several studies reported that BBB disruption plays a pivotal role in AD pathology [56,57] and suggested that its breakdown is an early event in advanced-aged human brains and contributes to cognitive decline [58]. Findings from our study indicate that EVOO- and OC-enriched diets increased BBB's tightness through significant upregulation of tight and adherence junction proteins. At the doses administered, while EVOO induced the expression of claudin-5 and occludin, OC induced VE-cadherin. Compared with our previous findings with OC-rich EVOO, which demonstrated a significant increase in claudin-5 expression [30,31], the current data suggest that the induced reported increase in claudin-5 could be mediated by EVOO-phenols, and not OC.

Increased A β levels in the brains of AD patients could be initiated by the imbalance between A β production and its clearance, which subsequently could lead to brain A β accumulation [59,60]. Here, we examined the effect of OC-low EVOO and OC on brain A β ,

proteins involved in its clearance across the BBB, and proteins related to its production. While the obtained results are consistent with our previous reports, they also suggested a lack of difference between EVOO and OC for their effect on A β production and clearance across the BBB. EVOO and OC reduced total A β , A β deposits, and soluble A β_{40} and A β_{42} . Such a decrease in A β was associated with increased expression of P-gp and LRP1, implying improved BBB function. In addition, EVOO and OC reduced the production of A β by shifting the processing of APP toward the non-amyloidogenic pathway. This effect was associated with a significant reduction in sAPP β . These findings are consistent with our previous studies reporting that OC-rich EVOO significantly elevated sAPP α and ADAM10 in the AD mouse model TgSwDI [30].

There is tremendous evidence that neuroinflammation is a crucial factor in AD pathology. Under normal physiological conditions, glial cells have a phagocytic function [61]. However, in AD brains, glial cells become activated and secrete several proinflammatory cytokines, such as IL-6, IL-1 β , and TNF- α , and other oxidative stress markers, eventually leading to neuronal death [61]. EVOO and OC reduced astrocyte activation as demonstrated by GFAP and cytokines levels. To clarify the affected neuroinflammatory pathway(s) that played a role in the observed effect, at least in part, we assessed NLRP3 inflammasome and RAGE/HMGB1 pathways, both of which are mediated by NF- κ B pathway activation. Advance glycated end-products (AGEs) up-regulation has been associated with aging and neurodegenerative diseases, including AD [62–64]. In AD, the level of AGEs is significantly higher when compared with normal brains [65,66]. In addition, RAGE is highly expressed in activated astrocytes. RAGE is also expressed in different brain cells, including endothelial cells of the BBB, neurons, and microglia [65]. Ligands such as A β and HMGB1 proteins have been shown to interact and increase the expression and activity of RAGE [67–70]. HMGB1 release from various cells, including astrocytes and microglia, contributes to AD via its binding to RAGE, which activates inflammatory responses [71,72]. Upon interactions, A β and HMGB1 activate the NF- κ B pathway [73–75]. RAGE induced-activation of NF- κ B promotes the expression of proinflammatory cytokines, which induces a prolonged activation and promotion of signaling mechanisms for cell damage and regulates NLRP3 inflammasome activation [76–78]. Furthermore, HMGB1 and A β could directly induce NLRP3 activation and promote the formation of the inflammasome complex, which results in the activation of caspase 1 and caspase 8 and the production of proinflammatory cytokines IL-1 β , IL-6, and IL-18 [76,79]. The activation of NLRP3 inflammasomes enhances AD progression by mediating chronic inflammatory responses [77], which are partly involved in restricting glial function, and mediating synaptic dysfunction and cognitive impairment [77], as well as BBB dysfunction [80]. Therefore, blocking RAGE and NLRP3 inflammasome activation could effectively interfere with the progression of AD. Our study findings demonstrated that only OC suppressed RAGE/HMGB1 pathway, while OC-low EVOO did not alter this pathway. In addition, the effect of OC on NLRP3 inflammasome suppression was significantly greater than that of OC-low EVOO. In the brains of EVOO- and OC-treated mice, IL-1 β levels were significantly decreased when compared with the ROO group. This effect was associated with a significant reduction in the expression of two major pro-caspases responsible for the increased formation of IL-1 β via the activation of caspase-1 [81] and caspase-8 [82]. Reduced neuroinflammation by both EVOO and OC was associated with a comparable reduction in the NF- κ B pathway.

Besides OC, EVOO contains many other phenolic compounds. Among the most studied EVOO-phenols for their effect against AD pathology are hydroxytyrosol, tyrosol, oleuropein, oleacein, and luteolin [39–48]. Findings from in vitro and in vivo studies with these phenols demonstrated their effect against A β and related pathology, where they were able to reduce A β levels by blocking A β aggregation, reduce A β production, and increase its clearance by different mechanisms, including autophagy and across the BBB. Furthermore, EVOO-phenols, including OC, reduced oxidative stress and neuroinflammation by targeting nuclear factor erythroid 2-related factor 2 (NRF2), nitric oxide (NO), Janus kinase/signal transducer and activator of transcription (JAK/STAT), and mitogen-activated

protein kinase (MAPK) signaling pathways, to list a few, which could synergistically or additively alleviate AD pathology [39–48]. The phenols mentioned above exist in the EVOO examined in this study. When tested at an equivalent dose to ROO spiked with OC (0.5 mg/kg), both demonstrated comparable effects against A β pathology.

This study has a few limitations. First is the lack of behavioral studies to compare the effect of EVOO and OC on memory function. Other limitations include the lack of a control group that did not receive any olive oil and the use of male-only mice in the study. Indeed, additional studies are necessary to confirm our findings and to assess and compare different olive oils with different phenolic content.

In conclusion, our findings confirm previously reported results on EVOO and OC to prevent and/or treat AD. In addition, and for the first time, our findings demonstrate that compared to ROO, at equivalent doses, OC-low EVOO and OC effectively reduced A β and related pathology. Furthermore, we showed that low doses of EVOO phenolics and OC could positively impact AD-related pathology. Both EVOO and OC reduced neuroinflammation by suppressing NLRP3 inflammasomes and NF- κ B pathways. In comparison, OC demonstrated an additional effect by suppressing RAGE/HMGB1 pathway. Collectively, our current and previous findings implicate that diet supplementation with EVOO low (but containing other phenols) or rich in OC could have a beneficial effect against AD.

4. Materials and Methods

4.1. Materials

Western blotting reagents, including buffers and gels, were obtained from Bio-Rad Laboratories (Hercules, CA, USA). NP-40 lysis buffer and 4x Laemmle sample buffer were purchased from Alfa Aesar (Haverhill, MA, USA). ThioS, bovine serum albumin (BSA), and donkey serum were purchased from Sigma-Aldrich (St. Louis, MO, USA). Non-fat dry milk was purchased from Santa Cruz Biotechnology (Dallas, TX, USA). Protease inhibitor and FemtoLUCENT™ PLUS-HRP were obtained from G-Biosciences (St. Louis, MO, USA). Pierce ECL WB substrate was purchased from Thermo-Fisher Scientific (Waltham, MA, USA). All other chemicals were purchased from VWR (Radnor, PA, USA) or Fisher Scientific (Hampton, NH, USA). Antibodies used for Western blot (WB) and IHC are summarized in Table 1.

Table 1. List of antibodies.

Antibody	Company
Western blot	
Anti-mouse IgG (H+L) secondary antibody, HRP-labeled	Invitrogen (Waltham, MA, USA)
Anti-rabbit IgG (H+L) secondary antibody, HRP-labeled	Invitrogen
ADAM10	Santa Cruz Biotechnology (Dallas, TX, USA)
Claudin-5	Invitrogen
GAPDH	Invitrogen
HMGB1	Santa Cruz Biotechnology
I κ B- α	Cell Signaling (Danvers, MA, USA)
LRP1	Abcam (Waltham, MA, USA)
NLRP3	Cell Signaling
Occludin	Invitrogen
p- I κ B- α	Cell Signaling
P-gp	BioLegend (San Diego, CA, USA)
p-IKK	Cell Signaling
Pro-caspase 1	Santa Cruz Biotechnology

Table 1. *Cont.*

Antibody	Company
Pro-caspase 8	Santa Cruz Biotechnology
PSD-95	Invitrogen
RAGE	Santa Cruz Biotechnology
sAPP- α	IBL America (Minneapolis, MN, USA)
sAPP- β	IBL America
SNAP-25	Invitrogen
Synapsin-1	Cell Signaling
VE-cadherin	Santa Cruz Biotechnology
Immunofluorescence staining	
Alexa-fluor 488-labeled 6E10	BioLegend
Anti-goat IgG–CFL594	Santa Cruz Biotechnology
Anti-goat HRP-labeled secondary	R&D Systems (Minneapolis, MN, USA)
Anti-collagen-IV	EDM-Millipore (Burlington, MA, USA)
Anti-rabbit IgG-CFL594	Santa Cruz Biotechnology
GFAP	Santa Cruz Biotechnology

4.2. Animals

All animal experiments and procedures were approved by the Institutional Animal Care and Use Committee of Auburn University and according to the National Institutes of Health guidelines. The mouse model used for this study is the homozygous 5xFAD mouse. The heterozygous 5xFAD mouse model rapidly develops severe A β -related pathology and accumulates high levels of A β , beginning around 1.5 months of age [83]. Astrogliosis and microgliosis develop parallel with A β plaque deposition at approximately two months of age. 5xFAD mice develop an APP gene dosage-dependent aggravation of the neurological phenotype. Compared to the heterozygous mice, homozygous 5xFAD mice develop amyloid pathology much more rapidly with an aggravated neuropathological and behavioral phenotype [84]. The homozygous 5xFAD mice were produced by breeding heterozygous 5xFAD (Jackson Laboratory; Bar Harbor, ME), and the offspring were confirmed by genotyping. The mice were housed in plastic containers under standard conditions, 12-h light/dark cycle, 22 °C, and 35% relative humidity, with ad libitum access to water and food. For the experiments, mice received EVOO- and OC-enriched diet for 3 months starting at the age of 3 months.

Male 5xFAD mice were divided into three groups (n = 10 mice/group). Group 1 received ROO (containing <10 mg/kg total biophenols; vehicle group) mixed with a regular powdered diet (Teklad Laboratory diets, Harlan Laboratories, Madison, WI, USA); group 2 received EVOO mixed with the powdered food; and group 3 received OC spiked in the refined olive oil that was then mixed with the powdered food. The phenolic compounds present in the EVOO and their concentrations are listed in Table 2. For the studies, EVOO that is low in OC was used with total phenolic content of 540 mg/kg, with OC presenting less than 35 mg/kg. For group 3 treatment, OC was spiked at 540 mg/kg in olive oil to produce a concentration equivalent to the total phenols in the EVOO used in this study. The olive oils were obtained from Boundary Bend Olive Pty (Australia). ROO-, EVOO- and OC-enriched diets were prepared based on the dietary intake of olive oil in the Greek population, that is 50 g/day [85], which resulted in a daily dose of 0.5 mg/kg body weight of total phenols (in EVOO) and OC. Mice were fed with ROO-, EVOO- and OC-enriched diet beginning at three months and continued for three months to end the treatment at six months. The enriched diet was changed every day to maintain freshness.

Table 2. Phenolic compounds and their concentrations present in EVOO.

Biophenols (mg/kg)	ROO	EVOO
Hydroxytyrosol		5.1
Tyrosol		3.1
Vanillic acid and Caffeic acid		1.8
Vanillin		1.5
Para-coumaric acid		2.7
Ferulic acid		4.2
Decarboxymethyl oleuropein aglycone oxidized dialdehyde form		34.1
Oleacein		85.2
Oleuropein		29.9
Oleuropein aglycone, dialdehyde form		49.3
Tyrosol acetate		24.9
Decarboxymethyl ligstroside aglycone, oxidised dialdehyde form		37.1
Oleocanthal		33.9
Cinnamic acid		59.1
Ligstroside aglycone, dialdehyde form		12.7
Oleuropein aglycone, oxidized aldehyde, and hydroxylic form		17.4
Luteolin		36
Oleuropein aglycone, aldehyde, and hydroxylic form		58.2
Ligstroside aglycone, oxidised aldehyde, and hydroxylic form		15.1
Apigenin		16.6
Ligstroside aglycone, aldehyde and hydroxylic form		11.4
Total biophenol content mg/kg	<10	539.3

4.3. Western Blot Analysis

Brain tissues were collected and homogenized, as reported previously [46]. Briefly, brain tissues were lysed with NP-40 lysis buffer containing 1x protease inhibitors followed by centrifugation at $20,800 \times g$ for 20 min at 4 °C. The supernatant was collected and stored at -80 °C until use for analysis. Pierce BCA Protein Assay kit was used to quantify the total protein content.

For Western blotting, 30 μ g of sample protein were loaded and resolved on 10% SDS-polyacrylamide gel, then transferred electrophoretically onto PVDF membranes. Membranes were blocked using 1% milk for 1 h at room temperature; membranes were then incubated overnight at 4 °C with primary antibodies. Primary antibodies used for immunolabeling are listed in Table 1. For detection, HRP-labeled secondary antibodies were used (Table 1). The bands were visualized using the ChemiDoc MP Imaging System (Bio-Rad). The immunoreactive bands were quantified by densitometric analysis using Image Lab Software V.6.0 (Bio-Rad). The results were expressed as a fold change in protein level compared to the ROO group after normalization to the housekeeping proteins.

4.4. Immunofluorescence Staining and Analysis

Brain cryosections of 16 μ m-thick were prepared by ThermoScientific™ HM525 NX Cryostat (Waltham, MA, USA). We used a similar staining protocol to our previous studies [46]. In brief, brain sections were fixed with methanol at -20 °C for 10 min, followed by washing with phosphate-buffered saline and blocking with 10% donkey serum for 1 h at room temperature. Primary and secondary antibodies used for these experiments are listed in Table 1. The brain sections were double stained with Alexa Fluor 488 labeled 6E10 human specific anti-A β antibody (1:1000 dilution) to detect total A β , and rabbit polyclonal collagen IV antibody (1:200) to detect brain microvessels for 2 h followed by the donkey polyclonal Alexa Fluor 647 antibody to rabbit IgG (1:200). To detect A β plaques, brain sections were stained with a freshly prepared and filtered 0.02% ThioS solution in 70% ethanol for 30 min. Sections were washed in 70% ethanol for 15 min and covered with coverslips for imaging. To detect reactive astrocytes, sections were stained with rabbit anti-GFAP polyclonal IgG

(1:100) followed by anti-rabbit IgG—CFL594 secondary antibody. Fluorescent images were captured using a Nikon Eclipse TiS inverted fluorescence microscope (Melville, NY).

4.5. Enzyme-Linked Immunosorbent Assay (ELISA)

Soluble A β ₄₀ and A β ₄₂ levels in brain homogenates were quantified using commercially available ELISA kits according to the manufacturer's instructions (R&D Systems). In addition to A β , the proinflammatory cytokines IL-1 β and IL-6 levels in mice brain homogenates were determined using ELISA according to the manufacturer's instructions (R&D Systems). All samples were run at least in duplicate and corrected to the total protein amount in each sample using the BCA assay.

4.6. Statistical Analysis

Data analysis was performed using GraphPad Prism v5.0 software. The experimental results were statistically analyzed for the significant difference using Student's t-test. All *p* values were statistically significant at *p* < 0.05. The results are presented as mean \pm SEM.

Author Contributions: I.M.A. performed the experiments and data analysis and wrote the manuscript; K.M.A.-S. performed the experiments and contributed to the manuscript review; A.E.A. and N.F.A.-G. performed the data analysis and contributed to the manuscript writing and review; C.G. contributed to designing the experiments and manuscript review; A.K. contributed to designing the experiments, writing, reviewing, editing the manuscript, and funding acquisition. All authors have read and agreed to the published version of the manuscript.

Funding: This research was funded by Boundary Bend Olives Pty, Australia.

Institutional Review Board Statement: The study was conducted according to the guidelines of the Declaration of Helsinki and approved by the Institutional Animal Care and Use Committee of Auburn University (protocol code 2018-3296, date of approval 7 May 2018).

Data Availability Statement: The data presented in this study are available within the article text and figures.

Conflicts of Interest: The authors declare no conflict of interest. The corresponding author, Amal Kaddoumi, is a co-founder and equity shareholder in Oleolive, LLC. The funders had no role in the design of the study; in the collection, analyses, or interpretation of data; in the writing of the manuscript, or in the decision to publish the results.

Sample Availability: ROO, EVOO and OC are commercially available.

References

1. Breijyeh, Z.; Karaman, R. Comprehensive review on Alzheimer's disease: Causes and treatment. *Molecules* **2020**, *25*, 5789. [[CrossRef](#)] [[PubMed](#)]
2. Mebane-Sims, I. Alzheimer's Association, 2018 Alzheimer's disease facts and figures. *Alzheimer's Dement* **2018**, *14*, 367–429.
3. Adav, S.S.; Sze, S.K. Insight of brain degenerative protein modifications in the pathology of neurodegeneration and dementia by proteomic profiling. *Mol. Brain* **2016**, *9*, 1–22. [[CrossRef](#)] [[PubMed](#)]
4. Murphy, M.; LeVine III, H. Alzheimer's disease and the β -amyloid peptide. *J. Alzheimer's Dis* **2010**, *19*, 311–323. [[CrossRef](#)] [[PubMed](#)]
5. Alzheimer's Association. 2019 Alzheimer's disease facts and figures. *Alzheimer's Dement* **2019**, *15*, 321–387. [[CrossRef](#)]
6. Long, J.M.; Holtzman, D.M. Alzheimer disease: An update on pathobiology and treatment strategies. *Cell* **2019**, *179*, 312–339. [[CrossRef](#)]
7. DeTure, M.A.; Dickson, D.W. The neuropathological diagnosis of Alzheimer's disease. *Mol. Neurodegener.* **2019**, *14*, 1–18. [[CrossRef](#)]
8. O'Brien, R.J.; Wong, P.C. Amyloid precursor protein processing and Alzheimer's disease. *Annu. Rev. Neurosci.* **2011**, *34*, 185–204. [[CrossRef](#)]
9. Chen, G.-f.; Xu, T.-h.; Yan, Y.; Zhou, Y.-r.; Jiang, Y.; Melcher, K.; Xu, H.E. Amyloid beta: Structure, biology and structure-based therapeutic development. *Acta Pharmacol. Sin.* **2017**, *38*, 1205–1235. [[CrossRef](#)]
10. Tillement, L.; Lecanu, L.; Papadopoulos, V. Alzheimer's disease: Effects of β -amyloid on mitochondria. *Mitochondrion* **2011**, *11*, 13–21. [[CrossRef](#)]
11. Holtzman, D.M.; Morris, J.C.; Goate, A.M. Alzheimer's disease: The challenge of the second century. *Sci. Transl. Med.* **2011**, *3*, 77sr71. [[CrossRef](#)]

12. Kinney, J.W.; Bemiller, S.M.; Murtishaw, A.S.; Leisgang, A.M.; Salazar, A.M.; Lamb, B.T. Inflammation as a central mechanism in Alzheimer's disease. *Alzheimer's Dement. Transl. Res. Clin. Interv.* **2018**, *4*, 575–590. [[CrossRef](#)]
13. Zotova, E.; Nicoll, J.A.; Kalaria, R.; Holmes, C.; Boche, D. Inflammation in Alzheimer's disease: Relevance to pathogenesis and therapy. *Alzheimer's Res. Ther.* **2010**, *2*, 1. [[CrossRef](#)]
14. Onyango, I.G.; Jauregui, G.V.; Čarná, M.; Bennett, J.P., Jr.; Stokin, G.B. Neuroinflammation in Alzheimer's disease. *Biomedicines* **2021**, *9*, 524. [[CrossRef](#)]
15. Yoon, S.-S.; Jo, S.A. Mechanisms of amyloid- β peptide clearance: Potential therapeutic targets for Alzheimer's disease. *Biomol. Ther.* **2012**, *20*, 245. [[CrossRef](#)]
16. Zhang, G.; Wang, Z.; Hu, H.; Zhao, M.; Sun, L. Microglia in Alzheimer's Disease: A Target for Therapeutic Intervention. *Front. Cell. Neurosci.* **2021**, *15*, 749587. [[CrossRef](#)]
17. Uddin, M.S.; Kabir, M.T.; Al Mamun, A.; Barreto, G.E.; Rashid, M.; Perveen, A.; Ashraf, G.M. Pharmacological approaches to mitigate neuroinflammation in Alzheimer's disease. *Int. Immunopharmacol.* **2020**, *84*, 106479. [[CrossRef](#)]
18. Saha, R.N.; Pahan, K. Regulation of inducible nitric oxide synthase gene in glial cells. *Antioxid. Redox Signal.* **2006**, *8*, 929–947. [[CrossRef](#)]
19. Morgan, M.J.; Liu, Z.-g. Crosstalk of reactive oxygen species and NF- κ B signaling. *Cell Res.* **2011**, *21*, 103–115. [[CrossRef](#)]
20. Hensley, K. Neuroinflammation in Alzheimer's disease: Mechanisms, pathologic consequences, and potential for therapeutic manipulation. *J. Alzheimer's Dis.* **2010**, *21*, 1–14. [[CrossRef](#)]
21. Abbott, N.J.; Patabendige, A.A.; Dolman, D.E.; Yusof, S.R.; Begley, D.J. Structure and function of the blood–brain barrier. *Neurobiol. Dis.* **2010**, *37*, 13–25. [[CrossRef](#)] [[PubMed](#)]
22. Wisniewski, H.M.; Vorbrodt, A.W.; Wegiel, J. Amyloid Angiopathy and Blood–Brain Barrier Changes in Alzheimer's Disease a, b. *Ann. N. Y. Acad. Sci.* **1997**, *826*, 161–172. [[CrossRef](#)] [[PubMed](#)]
23. Cirrito, J.R.; Deane, R.; Fagan, A.M.; Spinner, M.L.; Parsadanian, M.; Finn, M.B.; Jiang, H.; Prior, J.L.; Sagare, A.; Bales, K.R. P-glycoprotein deficiency at the blood-brain barrier increases amyloid- β deposition in an Alzheimer disease mouse model. *J. Clin. Investig.* **2005**, *115*, 3285–3290. [[CrossRef](#)] [[PubMed](#)]
24. Qosa, H.; Abuasal, B.S.; Romero, I.A.; Weksler, B.; Couraud, P.-O.; Keller, J.N.; Kaddoumi, A. Differences in amyloid- β clearance across mouse and human blood–brain barrier models: Kinetic analysis and mechanistic modeling. *Neuropharmacology* **2014**, *79*, 668–678. [[CrossRef](#)]
25. Scarmeas, N.; Stern, Y.; Tang, M.X.; Mayeux, R.; Luchsinger, J.A. Mediterranean diet and risk for Alzheimer's disease. *Ann. Neurol. Off. J. Am. Neurol. Assoc. Child Neurol. Soc.* **2006**, *59*, 912–921. [[CrossRef](#)]
26. Gu, Y.; Nieves, J.W.; Stern, Y.; Luchsinger, J.A.; Scarmeas, N. Food combination and Alzheimer disease risk: A protective diet. *Arch. Neurol.* **2010**, *67*, 699–706. [[CrossRef](#)]
27. Roman, G.C.; Jackson, R.; Reis, J.; Román, A.; Toledo, J.; Toledo, E. Extra-virgin olive oil for potential prevention of Alzheimer disease. *Rev. Neurol.* **2019**, *175*, 705–723. [[CrossRef](#)]
28. Abuznait, A.H.; Qosa, H.; Busnena, B.A.; El Sayed, K.A.; Kaddoumi, A. Olive-oil-derived oleocanthal enhances β -amyloid clearance as a potential neuroprotective mechanism against Alzheimer's disease: In vitro and in vivo studies. *ACS Chem. Neurosci.* **2013**, *4*, 973–982. [[CrossRef](#)]
29. Qosa, H.; Mohamed, L.A.; Batarseh, Y.S.; Alqahtani, S.; Ibrahim, B.; LeVine III, H.; Keller, J.N.; Kaddoumi, A. Extra-virgin olive oil attenuates amyloid- β and tau pathologies in the brains of TgSwDI mice. *J. Nutr. Biochem.* **2015**, *26*, 1479–1490. [[CrossRef](#)]
30. Al Rihani, S.B.; Darakjian, L.I.; Kaddoumi, A. Oleocanthal-rich extra-virgin olive oil restores the blood–brain barrier function through NLRP3 inflammasome inhibition simultaneously with autophagy induction in TgSwDI mice. *ACS Chem. Neurosci.* **2019**, *10*, 3543–3554. [[CrossRef](#)]
31. Batarseh, Y.S.; Kaddoumi, A. Oleocanthal-rich extra-virgin olive oil enhances donepezil effect by reducing amyloid- β load and related toxicity in a mouse model of Alzheimer's disease. *J. Nutr. Biochem.* **2018**, *55*, 113–123. [[CrossRef](#)]
32. Kaddoumi, A.; Denney, T.S., Jr.; Deshpande, G.; Robinson, J.L.; Beyers, R.J.; Redden, D.T.; Praticò, D.; Kyriakides, T.C.; Lu, B.; Kirby, A.N. Extra-Virgin Olive Oil Enhances the Blood–Brain Barrier Function in Mild Cognitive Impairment: A Randomized Controlled Trial. *Nutrients* **2022**, *14*, 5102. [[CrossRef](#)]
33. Tsolaki, M.; Lazarou, E.; Kozori, M.; Petridou, N.; Tabakis, I.; Lazarou, I.; Karakota, M.; Saoulidis, I.; Melliou, E.; Magiatis, P. A randomized clinical trial of greek high phenolic early harvest extra virgin olive oil in mild cognitive impairment: The MICOIL pilot study. *J. Alzheimer's Dis.* **2020**, *78*, 801–817. [[CrossRef](#)]
34. Tripoli, E.; Giammanco, M.; Tabacchi, G.; Di Majo, D.; Giammanco, S.; La Guardia, M. The phenolic compounds of olive oil: Structure, biological activity and beneficial effects on human health. *Nutr. Res. Rev.* **2005**, *18*, 98–112. [[CrossRef](#)]
35. Reboredo-Rodríguez, P.; Varela-López, A.; Forbes-Hernández, T.Y.; Gasparrini, M.; Afrin, S.; Cianciosi, D.; Zhang, J.; Manna, P.P.; Bompadre, S.; Quiles, J.L.; et al. Phenolic Compounds Isolated from Olive Oil as Nutraceutical Tools for the Prevention and Management of Cancer and Cardiovascular Diseases. *Int. J. Mol. Sci.* **2018**, *19*, 2305. [[CrossRef](#)]
36. Rodríguez-Morató, J.; Xicota, L.; Fitó, M.; Farré, M.; Dierssen, M.; De la Torre, R. Potential role of olive oil phenolic compounds in the prevention of neurodegenerative diseases. *Molecules* **2015**, *20*, 4655–4680. [[CrossRef](#)]
37. Beauchamp, G.K.; Keast, R.S.; Morel, D.; Lin, J.; Pika, J.; Han, Q.; Lee, C.-H.; Smith, A.B.; Breslin, P.A. Ibuprofen-like activity in extra-virgin olive oil. *Nature* **2005**, *437*, 45–46. [[CrossRef](#)]

38. Qosa, H.; Batarseh, Y.S.; Mohyeldin, M.M.; El Sayed, K.A.; Keller, J.N.; Kaddoumi, A. Oleocanthal enhances amyloid- β clearance from the brains of TgSwDI mice and in vitro across a human blood-brain barrier model. *ACS Chem. Neurosci.* **2015**, *6*, 1849–1859. [[CrossRef](#)]
39. Romero-Márquez, J.M.; Navarro-Hortal, M.D.; Jiménez-Trigo, V.; Muñoz-Ollero, P.; Forbes-Hernández, T.Y.; Esteban-Muñoz, A.; Giampieri, F.; Delgado Noya, I.; Bullón, P.; Vera-Ramírez, L. An Olive-Derived Extract 20% Rich in Hydroxytyrosol Prevents β -Amyloid Aggregation and Oxidative Stress, Two Features of Alzheimer Disease, via SKN-1/NRF2 and HSP-16.2 in *Caenorhabditis elegans*. *Antioxidants* **2022**, *11*, 629. [[CrossRef](#)]
40. Leri, M.; Bertolini, A.; Stefani, M.; Bucciantini, M. EVOO Polyphenols Relieve Synergistically Autophagy Dysregulation in a Cellular Model of Alzheimer's Disease. *Int. J. Mol. Sci.* **2021**, *22*, 7225. [[CrossRef](#)]
41. Delgado, A.; Cholevas, C.; Theoharides, T.C. Neuroinflammation in Alzheimer's disease and beneficial action of luteolin. *Biofactors* **2021**, *47*, 207–217. [[CrossRef](#)]
42. Qin, C.; Hu, S.; Zhang, S.; Zhao, D.; Wang, Y.; Li, H.; Peng, Y.; Shi, L.; Xu, X.; Wang, C. Hydroxytyrosol Acetate Improves the Cognitive Function of APP/PS1 Transgenic Mice in ER β -dependent Manner. *Mol. Nutr. Food Res.* **2021**, *65*, 2000797. [[CrossRef](#)] [[PubMed](#)]
43. Grewal, R.; Reutzel, M.; Dilberger, B.; Hein, H.; Zotzel, J.; Marx, S.; Tretzel, J.; Sarafeddin, A.; Fuchs, C.; Eckert, G.P. Purified oleocanthal and ligstroside protect against mitochondrial dysfunction in models of early Alzheimer's disease and brain ageing. *Exp. Neurol.* **2020**, *328*, 113248. [[CrossRef](#)] [[PubMed](#)]
44. Leri, M.; Natalello, A.; Bruzzone, E.; Stefani, M.; Bucciantini, M. Oleuropein aglycone and hydroxytyrosol interfere differently with toxic A β 1-42 aggregation. *Food Chem. Toxicol.* **2019**, *129*, 1–12. [[CrossRef](#)] [[PubMed](#)]
45. Nardiello, P.; Pantano, D.; Lapucci, A.; Stefani, M.; Casamenti, F. Diet supplementation with hydroxytyrosol ameliorates brain pathology and restores cognitive functions in a mouse model of amyloid- β deposition. *J. Alzheimer's Dis.* **2018**, *63*, 1161–1172. [[CrossRef](#)]
46. Abdallah, I.M.; Al-Shami, K.M.; Yang, E.; Wang, J.; Guillaume, C.; Kaddoumi, A. Oleuropein-Rich Olive Leaf Extract Attenuates Neuroinflammation in the Alzheimer's Disease Mouse Model. *ACS Chem. Neurosci.* **2022**, *13*, 1002–1013. [[CrossRef](#)]
47. Casamenti, F.; Grossi, C.; Rigacci, S.; Pantano, D.; Luccarini, I.; Stefani, M. Oleuropein aglycone: A possible drug against degenerative conditions. In vivo evidence of its effectiveness against Alzheimer's disease. *J. Alzheimer's Dis.* **2015**, *45*, 679–688. [[CrossRef](#)]
48. Castejón, M.L.; Montoya, T.; Ortega-Vidal, J.; Altarejos, J.; Alarcón-de-la-Lastra, C. Ligstroside aglycon, an extra virgin olive oil secoiridoid, prevents inflammation by regulation of MAPKs, JAK/STAT, NF- κ B, Nrf2/HO-1, and NLRP3 inflammasome signaling pathways in LPS-stimulated murine peritoneal macrophages. *Food Funct.* **2022**, *13*, 10200–10209. [[CrossRef](#)]
49. Citron, M. Alzheimer's disease: Strategies for disease modification. *Nat. Rev. Drug Discov.* **2010**, *9*, 387–398. [[CrossRef](#)]
50. Féart, C.; Samieri, C.; Barberger-Gateau, P. Mediterranean diet and cognitive function in older adults. *Curr. Opin. Clin. Nutr. Metab. Care* **2010**, *13*, 14–18. [[CrossRef](#)]
51. Hardman, R.J.; Kennedy, G.; Macpherson, H.; Scholey, A.B.; Pipingas, A. Adherence to a Mediterranean-style diet and effects on cognition in adults: A qualitative evaluation and systematic review of longitudinal and prospective trials. *Front. Nutr.* **2016**, *3*, 22. [[CrossRef](#)]
52. El Riachy, M.; Priego-Capote, F.; León, L.; Rallo, L.; Luque de Castro, M.D. Hydrophilic antioxidants of virgin olive oil. Part 1: Hydrophilic phenols: A key factor for virgin olive oil quality. *Eur. J. Lipid Sci. Technol.* **2011**, *113*, 678–691. [[CrossRef](#)]
53. Lauretti, E.; Iuliano, L.; Praticò, D. Extra-virgin olive oil ameliorates cognition and neuropathology of the 3xTg mice: Role of autophagy. *Ann. Clin. Transl. Neurol.* **2017**, *4*, 564–574. [[CrossRef](#)]
54. Lauretti, E.; Nenov, M.; Dincer, O.; Iuliano, L.; Praticò, D. Extra virgin olive oil improves synaptic activity, short-term plasticity, memory, and neuropathology in a tauopathy model. *Aging Cell* **2020**, *19*, e13076. [[CrossRef](#)]
55. Tzekaki, E.E.; Tsolaki, M.; Geromichalos, G.D.; Pantazaki, A.A. Extra Virgin Olive Oil consumption from Mild Cognitive Impairment patients attenuates oxidative and nitrative stress reflecting on the reduction of the PARP levels and DNA damage. *Exp. Gerontol.* **2021**, *156*, 111621. [[CrossRef](#)]
56. Zlokovic, B.V. Neurovascular pathways to neurodegeneration in Alzheimer's disease and other disorders. *Nat. Rev. Neurosci.* **2011**, *12*, 723–738. [[CrossRef](#)]
57. Baloyannis, S.J. Brain capillaries in Alzheimer's disease. *Hell. J. Nucl. Med.* **2015**, *18*, 152. [[CrossRef](#)]
58. Hawkins, B.T.; Davis, T.P. The blood-brain barrier/neurovascular unit in health and disease. *Pharmacol. Rev.* **2005**, *57*, 173–185. [[CrossRef](#)]
59. Hardy, J.A.; Higgins, G.A. Alzheimer's disease: The amyloid cascade hypothesis. *Science* **1992**, *256*, 184–185. [[CrossRef](#)]
60. Bates, K.; Verdile, G.; Li, Q.; Ames, D.; Hudson, P.; Masters, C.; Martins, R. Clearance mechanisms of Alzheimer's amyloid- β peptide: Implications for therapeutic design and diagnostic tests. *Mol. Psychiatry* **2009**, *14*, 469–486. [[CrossRef](#)]
61. Jung, Y.-J.; Chung, W.-S. Phagocytic roles of glial cells in healthy and diseased brains. *Biomol. Ther.* **2018**, *26*, 350. [[CrossRef](#)] [[PubMed](#)]
62. Sasaki, N.; Fukatsu, R.; Tsuzuki, K.; Hayashi, Y.; Yoshida, T.; Fujii, N.; Koike, T.; Wakayama, I.; Yanagihara, R.; Garruto, R. Advanced glycation end products in Alzheimer's disease and other neurodegenerative diseases. *Am. J. Pathol.* **1998**, *153*, 1149–1155. [[CrossRef](#)] [[PubMed](#)]

63. Galasko, D.; Bell, J.; Mancuso, J.Y.; Kupiec, J.W.; Sabbagh, M.N.; Van Dyck, C.; Thomas, R.G.; Aisen, P.S. Clinical trial of an inhibitor of RAGE-A β interactions in Alzheimer disease. *Neurology* **2014**, *82*, 1536–1542. [[CrossRef](#)] [[PubMed](#)]
64. Takeuchi, M.; Yamagishi, S. TAGE (toxic AGEs) hypothesis in various chronic diseases. *Med. Hypotheses* **2004**, *63*, 449–452. [[CrossRef](#)] [[PubMed](#)]
65. Takeuchi, M.; Yamagishi, S.-i. Possible involvement of advanced glycation end-products (AGEs) in the pathogenesis of Alzheimer's disease. *Curr. Pharm. Des.* **2008**, *14*, 973–978. [[CrossRef](#)]
66. Krautwald, M.; Münch, G. Advanced glycation end products as biomarkers and gerontotoxins—a basis to explore methylglyoxal-lowering agents for Alzheimer's disease? *Exp. Gerontol.* **2010**, *45*, 744–751. [[CrossRef](#)]
67. Yan, S.D.; Chen, X.; Fu, J.; Chen, M.; Zhu, H.; Roher, A.; Slattery, T.; Zhao, L.; Nagashima, M.; Morser, J. RAGE and amyloid- β peptide neurotoxicity in Alzheimer's disease. *Nature* **1996**, *382*, 685–691. [[CrossRef](#)]
68. Chen, J.; Song, M.; Yu, S.; Gao, P.; Yu, Y.; Wang, H.; Huang, L. Advanced glycation endproducts alter functions and promote apoptosis in endothelial progenitor cells through receptor for advanced glycation endproducts mediate overexpression of cell oxidant stress. *Mol. Cell. Biochem.* **2010**, *335*, 137–146. [[CrossRef](#)]
69. Chavakis, E.; Hain, A.; Vinci, M.; Carmona, G.; Bianchi, M.E.; Vajkoczy, P.; Zeiher, A.M.; Chavakis, T.; Dimmeler, S. High-mobility group box 1 activates integrin-dependent homing of endothelial progenitor cells. *Circ. Res.* **2007**, *100*, 204–212. [[CrossRef](#)]
70. Hofmann, M.A.; Drury, S.; Fu, C.; Qu, W.; Taguchi, A.; Lu, Y.; Avila, C.; Kambham, N.; Bierhaus, A.; Nawroth, P. RAGE mediates a novel proinflammatory axis: A central cell surface receptor for S100/calgranulin polypeptides. *Cell* **1999**, *97*, 889–901. [[CrossRef](#)]
71. Scaffidi, P.; Misteli, T.; Bianchi, M.E. Release of chromatin protein HMGB1 by necrotic cells triggers inflammation. *Nature* **2002**, *418*, 191–195. [[CrossRef](#)]
72. Bianchi, M.E.; Manfredi, A.A. High-mobility group box 1 (HMGB1) protein at the crossroads between innate and adaptive immunity. *Immunol. Rev.* **2007**, *220*, 35–46. [[CrossRef](#)]
73. Gao, H.-M.; Zhou, H.; Zhang, F.; Wilson, B.C.; Kam, W.; Hong, J.-S. HMGB1 acts on microglia Mac1 to mediate chronic neuroinflammation that drives progressive neurodegeneration. *J. Neurosci.* **2011**, *31*, 1081–1092. [[CrossRef](#)]
74. Son, M.; Lee, S.; Byun, K. Ligands receptor for advanced glycation end products produced by activated microglia are critical in neurodegenerative diseases. *J. Alzheimers Dis Park.* **2017**, *7*, 318. [[CrossRef](#)]
75. Mosquera, J.A. Role of the receptor for advanced glycation end products (RAGE) in inflammation. *Investig. Clin.* **2010**, *51*, 257–268.
76. Tan, M.-S.; Yu, J.-T.; Jiang, T.; Zhu, X.-C.; Tan, L. The NLRP3 inflammasome in Alzheimer's disease. *Mol. Neurobiol.* **2013**, *48*, 875–882. [[CrossRef](#)]
77. Heneka, M.T.; Kummer, M.P.; Stutz, A.; Delekate, A.; Schwartz, S.; Vieira-Saecker, A.; Griep, A.; Axt, D.; Remus, A.; Tzeng, T.-C. NLRP3 is activated in Alzheimer's disease and contributes to pathology in APP/PS1 mice. *Nature* **2013**, *493*, 674–678. [[CrossRef](#)]
78. Bauernfeind, F.G.; Horvath, G.; Stutz, A.; Alnemri, E.S.; MacDonald, K.; Speert, D.; Fernandes-Alnemri, T.; Wu, J.; Monks, B.G.; Fitzgerald, K.A. Cutting edge: NF- κ B activating pattern recognition and cytokine receptors license NLRP3 inflammasome activation by regulating NLRP3 expression. *J. Immunol.* **2009**, *183*, 787–791. [[CrossRef](#)]
79. Li, Q.; Chen, L.; Liu, X.; Li, X.; Cao, Y.; Bai, Y.; Qi, F. Pterostilbene inhibits amyloid- β -induced neuroinflammation in a microglia cell line by inactivating the NLRP3/caspase-1 inflammasome pathway. *J. Cell. Biochem.* **2018**, *119*, 7053–7062. [[CrossRef](#)]
80. Yang, F.; Wang, Z.; Wei, X.; Han, H.; Meng, X.; Zhang, Y.; Shi, W.; Li, F.; Xin, T.; Pang, Q. NLRP3 deficiency ameliorates neurovascular damage in experimental ischemic stroke. *J. Cereb. Blood Flow Metab.* **2014**, *34*, 660–667. [[CrossRef](#)]
81. Kaushal, V.; Dye, R.; Pakavathkumar, P.; Foveau, B.; Flores, J.; Hyman, B.; Ghetti, B.; Koller, B.; LeBlanc, A. Neuronal NLRP1 inflammasome activation of Caspase-1 coordinately regulates inflammatory interleukin-1-beta production and axonal degeneration-associated Caspase-6 activation. *Cell Death Differ.* **2015**, *22*, 1676–1686. [[CrossRef](#)]
82. Gurung, P.; Kanneganti, T.-D. Novel roles for caspase-8 in IL-1 β and inflammasome regulation. *Am. J. Pathol.* **2015**, *185*, 17–25. [[CrossRef](#)] [[PubMed](#)]
83. Oakley, H.; Cole, S.L.; Logan, S.; Maus, E.; Shao, P.; Craft, J.; Guillozet-Bongaarts, A.; Ohno, M.; Disterhoft, J.; Van Eldik, L. Intraneuronal β -amyloid aggregates, neurodegeneration, and neuron loss in transgenic mice with five familial Alzheimer's disease mutations: Potential factors in amyloid plaque formation. *J. Neurosci.* **2006**, *26*, 10129–10140. [[CrossRef](#)]
84. Richard, B.C.; Kurdakova, A.; Baches, S.; Bayer, T.A.; Weggen, S.; Wirths, O. Gene dosage dependent aggravation of the neurological phenotype in the 5xFAD mouse model of Alzheimer's disease. *J. Alzheimer's Dis.* **2015**, *45*, 1223–1236. [[CrossRef](#)] [[PubMed](#)]
85. Tuck, K.L.; Hayball, P.J. Major phenolic compounds in olive oil: Metabolism and health effects. *J. Nutr. Biochem.* **2002**, *13*, 636–644. [[CrossRef](#)] [[PubMed](#)]

Disclaimer/Publisher's Note: The statements, opinions and data contained in all publications are solely those of the individual author(s) and contributor(s) and not of MDPI and/or the editor(s). MDPI and/or the editor(s) disclaim responsibility for any injury to people or property resulting from any ideas, methods, instructions or products referred to in the content.